CHAPTER II
BACKGROUND AND LITERATURE SURVEY

2.1 Precipitation

When a solute concentration is below its saturation point, precipitation is not possible as refered to the stable zone in Figure 2.1. Thermodynamically, crystallization or precipitation is feasible once the solution becomes supersaturated at a given temperature. However, a certain supersaturation level is required before spontaneous crystallization occurs, as shown in Figure 2.1 by the dashed line in the solubility–supersaturation diagram. Below this level solutions appear to be stable or often referred to as "metastable" in the literature (Mullin, 1993). This metastability is attributable to slow precipitation kinetics. The mechanism of precipitation comprises two kinetic processes; nucleation, followed by crystal growth.

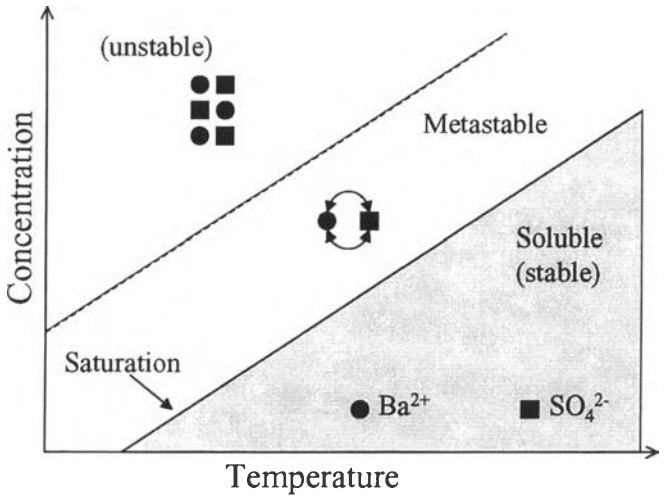

Figure 2.1 Solubility–supersaturation zones for barium sulphate: (i) undersaturated zone where barium sulphate is soluble and no precipitation is possible; (ii) metastable (supersaturated) zone where spontaneous precipitation is not likely; (iii) unstable zone where spontaneous precipitation is extremely likely to occur. (Mullin, 1993)

2.2 Nucleation

In a supersaturated solution the crystal ions associated into clusters by an addition mechanism that continues to grow until a critical size is reached. Below the critical size, the probability of the cluster existence is limited, therefore, these clusters typically redissolve. Whereas clusters above the critical size can exist to has stable "nuclei" and a new crystal surface. In the metastable zone in the supersaturated region, the nucleation rate is so low that precipitation is improbable within the measured time frame (middle zone in Figure 2.1) (Mullin, 1993 and Myerson, 1993). The width of this zone is given thermodynamically by the free energy of formation of the critical cluster size in homogenous nucleation. Homogeneous nucleation forms the basis of several nucleation theories and can be extended to heterogeneous nucleation. Two important parameters to characterize the nucleation process are: (i) the free energy change, and (ii) the rate of nuclei formation. In classical theory, the nucleation rate, that is the rate of nuclei formation, J (nuclei/cm^3 s), is given by an Arrhenius type of expression (Myerson, 1993):

$$J = A\exp\left[-\frac{\Delta G_{cr}}{k_B T}\right] \tag{2.1}$$

where A is the pre-exponential factor related to the efficiency of collisions of ions and molecules, which has a value of 10^{23}–10^{33} nuclei/cm^{3}sec, k_B the Boltzmann constant, T the absolute temperature, and ΔG_{cr} is the free energy change for the critical cluster size to form.

Classical theories of primary homogenous nucleation assume that, for supersaturated solutions, solute molecules combine to produce embryos. The overall free energy, ΔG, of the embryo is the sum of two terms; the free energy due to the formation of a new volume and the free energy due to the new surface created (Nielsen, 1964).

$$\Delta G = -\left(\frac{\beta_v r^3}{v}\right) k_B T \ln(S) + \gamma \beta_a r^2 \tag{2.2}$$

where ν is molecular volume of precipitated embryo, γ is the surface free energy per unit area ,β_v and β_a are volume and area shape factors, respectively. For a platelet nucleus, $\beta_v = 0.20$ and $\beta_a = 2.80$ (Myerson, 1993).

When the supersaturation ratio, $S<1.0$, $\Delta G(r)$ is always positive and the formation of a new phase will not occur. Alternatively, when the supersaturation ratio, $S>1.0$, $\Delta G(r)$ has a positive maximum at a critical size, r*, as shown in Figure 2.2. The height of the maximum in free energy curve is the activation energy for nucleation. Embryos larger than the critical size will further decrease their free energy by growth, giving "stable nuclei" which grow to form macroscopic particles. For the particles smaller than critical size will dissolve. This latter phenomenon is referred to as "ripening".

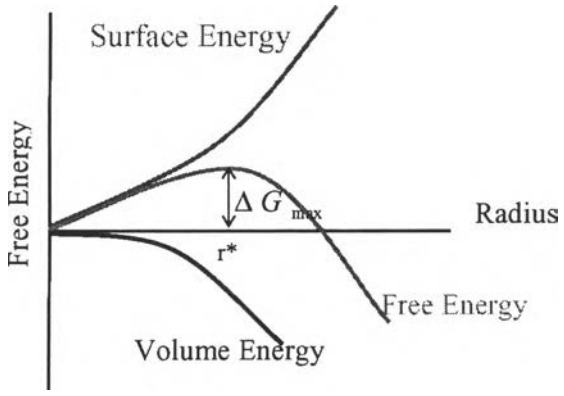

Figure 2.2 Classical nucleation theory: dependence of nuclear size on Gibbs free energy. (Myerson, 1993)

The critical nuclear size, r^*, can be obtained by setting $d\Delta G(r)/dr = 0$, giving

$$r^* = \frac{2\beta_a \gamma v}{3\beta_v k_B T \ln(S)} \qquad (2.3)$$

This critical size corresponds to the maximum of the free-energy curve, where ΔG_{max} is given by

$$\Delta G_{max} = \frac{\gamma \beta_a (r^*)^2}{3} \tag{2.4}$$

The nucleation rate can be expressed in molar quantities as well (Mullin, 1993):

$$J = A \exp\left[-\phi \beta_v \frac{\gamma^3 v^2}{(k_B T)^3 (\ln S)^2} \right] \tag{2.5}$$

where ϕ is the contact angle factor (unity for homogeneous nucleation).

The nucleation rate is critically dependent on supersaturation and temperature. As supersaturation increases the critical cluster size decreases as shown in Eq. (2.3). Similarly, a temperature increase will increase the nucleation rate as shown in Eq. (2.5) when S is kept constant. Thus, when supersaturation is increased, nucleation becomes increasingly favorable and nucleation occurs spontaneously, which is referred to as the metastable limit (upper broken line in Figure 2.1). Above this limit, solutions are unstable and immediate crystallization is likely to occur (Myerson, 1993).

2.3 Induction Time

The induction time, t_{ind}, is frequently used to estimate nucleation time and is defined as the time elapsed between the creation of supersaturation and the first appearance of the new crystal solid phase, ideally nuclei with the critical cluster size dimensions (Boerlage *et al.*, 2002). However, as the induction time is determined experimentally, it may also include growth to a detectable size. If it is assumed that the nucleation time is much greater than the time required for growth of crystal nuclei to a detectable size, then the induction time is inversely proportional to the rate of nucleation, $t_{ind} \propto J_n^{-1}$,i.e.:

$$t_{ind} = \frac{B}{J} \tag{2.6}$$

Eq. (2.5) can be written as

$$\ln t_{ind} = \frac{C}{(\log S)^2} - \ln \frac{B}{A} \tag{2.7}$$

With a plot of ln t_{ind} and $(\ln S)^{-2}$ at a constant temperature, the slope (C) will be obtained, where

$$C = \frac{-\phi \beta_v \gamma^3 v^2}{(kT)^3} \tag{2.8}$$

However, two linear regions may be observed in a plot covering a wide supersaturation range. The region of higher slope, visible at higher supersaturation ratios, corresponds to homogeneous nucleation while at lower supersaturation ratios a region of lower slope is a result of heterogeneous nucleation. The transition between these two regions may be smooth and connected by a continuous curve (Söhnel, 1992).

2.4 Supersaturation Ratio

The supersaturation of a system may be expressed in a number of different ways, and considerable confusion can arise if the conditions are not clearly defined. The temperature must also be specified. The supersatursation ratios is defined by Kashchiev (Kashchiev, 2003) dissociated into ions in solution, will be used in the present study as

$$S = \frac{[ATMP^{2-}][Ca^{2+}]}{K_{sp}} \tag{2.9}$$

where $[ATMP^{2-}]$ and $[Ca^{2+}]$ refer to concentrations of ATMP and calcium and K_{sp} is the equilibrium constant between the crystal ions in solution and the crystal solid phase (unity),i.e.

$$K_{sp} = [ATMP^{2-}]_e[Ca^{2+}]_e \quad \text{at equilibrium} \tag{2.10}$$

Where $[ATMP^{2-}]_e$ and $[Ca^{2+}]_e$ are equilibrium concentration of ATMP and calcium, respectively.

2.5 Crystal Growth

The overall crystal growth phenomenon consists of two processes in series: bulk diffusion through the mass transfer boundary layer, i.e. diffusion step, and incorporation of molecule into the crystal lattice, i.e. surface reaction step (Mullin, 1993). The rate of growth is expresses as

diffusion step : $$R_G = k_d(C_b - C_i) \tag{2.11}$$

surface reaction step : $$R_G = k_r(C_i - C^*)^r \tag{2.12}$$

overall growth : $$R_G = k_G(C_b - C^*)^g \tag{2.13}$$

where (C_b-C^*) is the driving force. A pictorial representation of these three stages is shown in Figure 2.3 where the various concentration driving forces can be seen. Crystals growing from solution can therefore be divided into diffusion dominant and surface reaction dominant. It is not possible to estimate the surface reaction order, r and the surface reaction rate constant, k_r without knowing the interface concentration of solute, C_i. Therefore, the interface concentration has to be estimated by combining Eq.(2.11) and Eq.(2.12) to obtain the general expression for the overall growth rate:

$$R_G = k_r\left[(C_b - C^*) - \frac{R_G}{k_d}\right]^r \tag{2.14}$$

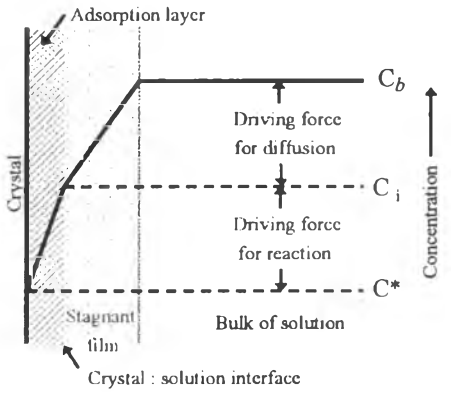

Figure 2.3 Concentration driving forces in crystallization from solution according to the simple diffusion-reaction model. (Mullin, 1993)

Two methods, the differential and integrated methods are mainly used for the measurements of the growth rates in experiments (Jibbouri, 2002). In this study, the differential method was used. In the differential method, the crystallization is seeded by adding a few grams of crystals with a known size into a supersaturated solution, where the crystal seeds grow. Because the amount of crystals added is small, it is assumed that the concentration of the solution does not change during the growth. The other assumptions are as follows:

1. There is no nucleation.
2. The number of crystal seeds put into the crystallizer is equal to the number of crystals taken out from the crystallizer.
3. There is no crystal loss.
4. All crystals have the same growth rate. If this assumption is not valid, the growth rates will need to be weight averaged.
5. The shape factors of the growing crystals are considered to be the same. This assumption is not always true especially in the case of surface nucleation. In this case, growth values are thought of as average values.

If the mass of the crystals put into and taken out from reactor are M_1 and M_2, respectively, they can be related to the size of the crystals L as:

$$M_1=N\beta_v\rho L_1^3, \tag{2.15}$$

$$M_2=N\beta_v\rho L_2^3, \tag{2.16}$$

where N is a number of crystals, L_1 and L_2 are the characteristic size of the crystals initially and at time t, respectively, β_v = 0.20 and ρ = 2.09 g/cm^3. The initial characteristic size was in the range of 3.75 – 5.50 μm. The overall linear growth rate G (m/s) is defined as the rate of the change of characteristic size:

$$G=\frac{\Delta L}{t} \tag{2.17}$$

By combining Eq.(2.16) and Eq.(2.17), one may express the growth rate in terms of size of the seed crystals and the weight of the crystals:

$$G=\frac{L_1}{t}\left[\left(\frac{M_2}{M_1}\right)^{1/3}-1\right] \tag{2.18}$$

G and R are related to each other as follows:

$$R=\frac{1}{A_c}\frac{dM}{dt}=\frac{1}{\beta_a L^2}\frac{d(\beta_v\rho L^3)}{dt}=\frac{3\beta_v\rho}{\beta_a}\frac{dL}{dt} \tag{2.19}$$

therefore

$$R=\frac{3\beta_v}{\beta_a}\rho G \tag{2.20}$$

where β_a is area shape factor = 2.80

These relationships will be useful in interpreting the experimental data.

2.6 Related Work

Lewis and Raju (1992) conducted a study on the squeeze treatment with the phosphonate, Aminotri(metrylene phosphonic acid) (ATMP). The reactivity of ATMP to precipitate with divalent cation species prevalent in typical brines, and secondly, the solubility of ATMP-cation precipitates was a function of pH, cation concentration, TDS and time. The matrix in the Middle Eastern oil producing formations is typically limestone in nature. It was concluded that the ATMP molecules were entirely feasible to construct the adsorption bonds with the limestone

formation matrix. This mechanism could function basically like a chromatography process and coupled with precipitation, resulting in very long return lifetimes.

Browning and Fogler (1996) studied the effects of changing precipitating conditions, the resuting properties of calcium-phosphonate precipitates were found to change significantly. The four major precipitate conditions affecting the properties of calcium-phosphonates were: the type of phophonate used, the pH of the precipitate solution, the calcium to phosphonate molar ratio of precipitating solution, and the degree of supersaturation of precipitate solution.`

Rerkpattanapipat (1996) studied the precipitation and dissolution of calcium –phosphonate (ATMP) on inhibition of scale formation in the porous media using the aminotri (metrylene phosphonic acid) (ATMP). The 3:1 Ca to ATMP molar ratio precipitate were found to be the best for actual squeeze treatments because it gave the longest squeeze lifetime. Furthermore, the squeeze lifetime was enhanced by adding excess calcium ion into the elution fluid (Wattana, 1997).

Veerapat (2003) studied the range of conditions under which Mg ions modulate the formation of Ca-ATMP precipitate. The results revealed that the amount of ATMP precipitated decreased with addition of Mg ions in the solution at all values of solution pH. Furthermore, an increase in both the solution pH and the concentration of the divalent cations in the solution resulted in a change of the molar ratio of (Ca+Mg) to ATMP in the precipitates. At a low solution pH (pH1.5), Mg ion had a little effect on the composition of the Ca-ATMP precipitate. However, at higher values of the solution pH (pH4 and 7), the Ca to ATMP molar ratio in the precipitates decreased with increasing concentration of Mg.